Many-Body Effects in the Excitation Spectrum of a Defect in SiC

Michel Bockstedte,[1,2] Andrea Marini,[3] Oleg Pankratov,[2] and Angel Rubio[1]

[1]*Nano-Bio Spectroscopy Group and ETSF Scientific Development Centre, Departamento Física de Materiales, Universidad del País Vasco, Centro de Física de Materiales CSIC-UPV/EHU-MPC and DIPC, Avenida Tolosa 72, E-20018 San Sebastián, Spain*

[2]*Lehrstuhl für Theoretische Festkörperphysik, Universität Erlangen-Nürnberg, Staudtstrasse 7 B2, D-91058 Erlangen, Germany*

[3]*European Theoretical Spectroscopy Facility (ETSF), Dipartimento di Fisica, Universitá di Roma Tor Vergata, I-0133 Roma, Italy*

(Received 15 February 2010; published 6 July 2010)

We show that electron correlations control the photophysics of defects in SiC through both renormalization of the quasiparticle band structure and excitonic effects. We consider the carbon vacancy with two possible excitation channels that involve conduction and valence bands. Corrections to the Kohn-Sham ionization levels strongly depend on the defect charge state. Excitonic effects introduce a redshift of 0.23 eV. The analysis reassigns excitation mechanism at the thresholds in photoinduced paramagnetic resonance measurements [J. Dashdorj *et al.*, J. Appl. Phys. **104**, 113707 (2008)].

DOI: 10.1103/PhysRevLett.105.026401 PACS numbers: 71.35.−y, 71.55.−i, 76.30.Mi

Optical spectra of semiconductors not only contain the excitations of the perfect bulk crystal but also that of its omnipresent imperfections, such as point defects. Photoluminescence plays a fundamental role in the experimental characterization and identification of defects [1]. Despite the success of density functional theory (DFT) in explaining the physics of defects in covalent semiconductors [2], this common approach has severe shortcomings: the description of the bonding of the bulk crystal may be insufficient within common approximations for exchange and correlation, like the local spin density approximation (LSDA), the position of defect levels in the band gap is affected by the well-known Kohn-Sham band gap error, and excitations cannot be assessed rigorously. Many-body perturbation theory allows one to resolve these issues [3], however, applications to defects are scarce [4] due to computational complexity. The quantitative prediction of absorption spectra of a wide class of systems from insulators to surfaces, to nanotubes and polymers became tractable only recently by solving the Bethe-Salpeter equations (BSE) and accounting for the G_0W_0 self-energy [3,5].

In electron paramagnetic resonance (EPR) experiments under illumination [6–8], the positively charged carbon vacancy (V_C^+) in the 4*H* polytype of silicon carbide (4*H*-SiC) was extensively investigated and excitation thresholds were assigned to the defect ionization levels with respect to the neutral defect. The identification of this defect as an EPR center was established on the basis of the DFT-LSDA ground state calculations [9,10]. Yet, for the accurate interpretation of the photo-EPR data one has to consider excitation transitions taking into account at least two competing excitation channels: transitions to the neutral state (V_C^0) as well as to the doubly positive defect (V_C^{2+}). To assess the values of the ionization levels one has to evaluate the contribution of excitonic effects that is unknown so far. Knowledge of the ionization levels is pivotal for an understanding of the carrier compensation in high purity semi-insulating SiC [11], in which vacancies are abundant compensation centers, and for the dopant diffusion and defect kinetics [12].

Defect excitations combine the many-body effects in both extended and localized states. The insertion of electrons into defect states invokes on-site correlation due to electron-electron repulsion expressed by the Hubbard *U*. Defect-to-band transitions involve two particles, the electron and the hole (one in the localized state and the other in the extended state). To self-energy effects this adds excitonic correlation energy of yet unknown size.

The aim of this Letter is to investigate many-body effects in the absorption spectrum of a well-identified defect: a carbon vacancy in 4*H*-SiC. We show that those corrections strongly depend on the occupation of the defect levels, indicating a Hubbard *U* which is substantially larger than predicted by DFT-LSDA (1.09 vs 0.79 eV). Furthermore excitonic effects introduce a sizeable redshift ($\sim$0.23 eV) varying with the defect charge state. More importantly, the calculated transition energy thresholds for the two competing channels indicate that the current interpretation of photo-EPR spectra [6–8] based on the assumption of a photoionization via the neutral defect has to be corrected. According to our calculations the ionization to V_C^{2+} is the only excitation mechanism at photon energies below 2.3 eV that is responsible for the experimental findings.

The defect absorption spectra and quasiparticle (QP) energies were investigated with the YAMBO-code [13]. The defect in 4*H*-SiC was represented by a supercell with 288 lattice sites [14]. Among the two inequivalent vacancy sites in 4*H*-SiC [9] we focus on the experimentally investigated cubic site. In the G_0W_0 and BSE calculations spin was taken into account [15]. First we turn to the fundamental band gap of 3*C*- and 4*H*-SiC. The QP cor-

rections using the DFT-lattice constant amount to 0.91 and 0.93 eV, respectively, in agreement with earlier G_0W_0 calculations [16]. Thereby, for the gap of 4H-SiC, we obtain 3.11 eV (the experimental value is 3.265 eV [17]).

Optical absorption, as indicated in Fig. 1, involves the defect levels in the band gap, a nondegenerate (a level) and a twofold degenerated level (e level). A (pseudo) Jahn-Teller effect [9] lifts the degeneracy for all charge states except for V_C^{2+}, however, for V_C^+ the effect is negligible. Electronic transitions occur predominantly at the fixed geometry of the initial state (Franck-Condon principle). The excitation threshold for transitions between the valence band (VB) and the defect states is determined by the QP energies of the lowest unoccupied defect state (LUMO) $\varepsilon_{\mathrm{LUMO}}^{\mathrm{QP}}$ and the valence band edge E_V and by the electron-hole (e-h) interaction E_{eh}, i.e., $\varepsilon_{\mathrm{LUMO}}^{\mathrm{QP}} - E_V - E_{\mathrm{eh}}$. For transitions from the highest occupied defect state (HOMO) to the conduction band (CB) with the band edge E_C the threshold is $E_C - \varepsilon_{\mathrm{HOMO}}^{\mathrm{QP}} - E_{\mathrm{eh}}$.

Ionization.—We now discuss the QP contribution to the threshold in comparison with the DFT values to discern the many-body corrections within the G_0W_0. The addition of an electron to the LUMO of the defect in the charge state q (V_C^q) yields V_C^{q-1}. Using E_V as an energy reference for the electron, the energy required for the addition is described by the QP-energy difference $\varepsilon_{\mathrm{LUMO}}^{\mathrm{QP}} - E_V$, which we denote $(q|q-1)_V$. Correspondingly, the removal of an electron from the HOMO of V_C^q, which yields V_C^{q+1}, is associated with the energy gain $\varepsilon_{\mathrm{HOMO}}^{\mathrm{QP}} - E_V$ denoted by $(q|q+1)_V$. In DFT, the values are obtained from the total energies. The results are listed in Table I. Consider first V_C^{2+} and V_C^+: for the electron addition to the unoccupied a level of V_C^{2+}, $(2+|+)_V$ obtained within G_0W_0 and DFT agree to within 20 meV. Also, for the electron removal from the a level of V_C^+, $(+|2+)_V$ obtained with G_0W_0 matches the DFT result. Hence, the addition (removal) of an unpaired electron to (from) the a level is already well described within DFT. Here the QP correction to the Kohn-Sham level of 0.2 eV (insertion) and −0.23 eV (removal) reflects electronic screening. However, for adding a second electron to the a level, exchange-correlation effects beyond the description of the DFT considerably change the mutual repulsion of the two electrons: the G_0W_0 value for $(+|0)_V$ is by 0.30 eV larger than the DFT result. The effective Hubbard interaction $U = (+|0)_V - (+|2+)_V$ (cf. [18]) among the two electrons in the QP treatment amounts to $U = 1.09$ eV instead of the DFT value $U = 0.79$ eV. For the remaining ionization levels, similar changes in the electron-electron repulsion due to the inclusion of exact exchange and the screened Coulomb-interaction in G_0W_0 beyond the DFT description are found.

The thermal ionization level $(q|q-1)$ determines in thermal equilibrium the positions of the Fermi level at which the charge state changes from q to $q-1$. The level $(q|q-1)$ differs from $(q|q-1)_V$ by the Franck-Condon shift, which is the energy gain due to the relaxation of the vacancy after electron insertion [cf. Figure 1(c)]. The relaxation leads to an effective electron-electron repulsion U_{eff} smaller than U. To assess $(q|q-1)$ within the G_0W_0 approach, we approximate the Franck-Condon shift E_{FC} by the DFT values. Results are listed in Table I. For V_C^+, DFT predicts a negative value for U_{eff} [18]. We obtain $U_{\mathrm{eff}} = -0.36$ eV. This would imply that in contradiction to findings [6,7] V_C^+ should hardly be observable by EPR in equilibrium. Yet, due to the QP corrections, the levels $(2+|+)$ and $(+|0)$ become almost equal (i.e., $U_{\mathrm{eff}} \approx 0$). This resolves the contradiction. For V_C^-, the negative-U effect persists after the QP correction ($U_{\mathrm{eff}} = -0.35$ eV).

Optical properties.—Photo-EPR experiments [6–8] were conducted with V_C^+ as the initial or the final state. The electronic transitions, that quench the paramagnetic state and include the ionization of V_C^+ into V_C^{2+} or V_C^0, are shown in Fig. 1: (i) excitation from the a level to the CB ($a \rightarrow C$), or (ii) from the VB to the defect levels a or e ($V \rightarrow a$ or $V \rightarrow e$). Restoring the EPR signal of V_C^+ starts from V_C^{2+} or V_C^0 as initial states by exciting an electron

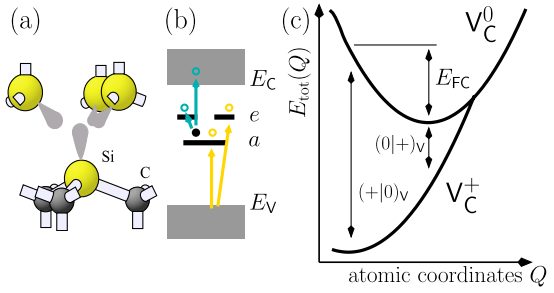

FIG. 1 (color online). Carbon vacancy V_C^+ in 4H-SiC: (a) geometry—the spin density is indicated, (b) defect levels within the band gap. In the ground state, the a level is occupied with the paramagnetic electron. Arrows indicate the transitions from the valence band (V) (lower set) and to the conduction band (C) (upper one). (c) sketch of the total energy $E_{\mathrm{tot}}(Q)$ of V_C^+ and V_C^0 vs the atomic coordinates; the QP-energies $(+|0)_V$ and $(0|+)_V$ and the Franck-Condon shift E_{FC} of V_C^0 are indicated (cf. text).

TABLE I. QP energies $(q|q+1)_V$ and $(q|q-1)_V$, Franck-Condon shifts E_{FC}, and thermal ionization levels $(q|q-1)$ for the relevant charge states of V_C in eV. Values are listed as obtained within G_0W_0 and DFT. First two columns: initial charge state with the occupation of its defect levels. E_{FC} is taken from DFT calculation after electron insertion (cf. text).

		$(q\|q+1)_V$		$(q\|q-1)_V$		E_{FC}	$(q\|q-1)$	
		G_0W_0	DFT	G_0W_0	DFT		G_0W_0	DFT
V_C^{2+}	a^0e^0			1.83	1.85	0.29	1.54	1.56
V_C^+	a^1e^0	1.27	1.24	2.36	2.03	0.83	1.53	1.20
V_C^0	a^2e^0	0.88	0.72	2.80	2.28	0.21	2.59	2.07
V_C^-	a^2e^1	1.76	1.39	2.65	2.16	0.41	2.24	1.76

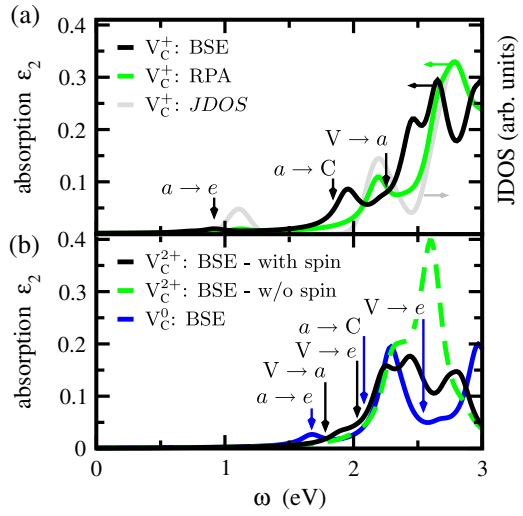

FIG. 2 (color online). Absorption spectra of V_C within G_0W_0-BSE: (a) for V_C^+ in comparison with the G_0W_0-RPA-spectrum and the joint density of states (JDOS) of the transitions with the a level, (b) for V_C^0 and V_C^{2+} as calculated with spin polarization and without (for the latter). The onset of excitation channels is indicated [19]. A broadening of 0.1 eV was used for all spectra.

from the VB to the a level (V_C^{2+}) or from the a level to the CB (V_C^0) and implies the subsequent dissociation of the e-h pair. We calculated absorption spectra for V_C^{2+}, V_C^+, and, V_C^0 to unravel the relevance of competing channels and to assess the e-h coupling. For the latter purpose we compared the spectra with the inclusion of the e-h interaction via the BSE and without it, in the random phase approximation (RPA). In the investigated energy range only absorption via defect states contributes to spectra due to the indirect band gap. The spectra are shown in Fig. 2 [19]. In Table II, we list the ionization and excitation thresholds as obtained from calculations using the special k point [14]. We also calculated RPA spectra, shown in Fig. 3, for the denser $4 \times 4 \times 4$ k-point mesh [20] that are converged with respect to the density of extended states. Since similar calculations are not feasible for the BSE, we extrapolated such BSE spectra by a convolution of the RPA spectra with kernels that convolute the corresponding RPA into BSE spectra of the special k point. Nonvertical transitions are accounted for by applying a Huang-Rhys factor for the coordinate that connects the geometry of the ground state and the ionized state (broadening amounts to ~0.26 eV).

First we address the spectra of V_C^+ obtained for the special k point [Fig. 2(a)]. Excitonic effects lead to an almost rigid redshift of the RPA spectrum by $E_{eh} = 0.23$ eV. The same effect is found also for V_C^{2+}, and V_C^0 albeit with different values of E_{eh} (cf. Table II). The RPA spectrum is dominated by band structure effects. This is demonstrated by comparison with the joint density of states (JDOS) of the transitions involving the a level, which essentially reproduces the RPA spectrum. The spectral broadening by Huang-Rhys factors reduces these features as seen in Fig. 3. Deviations between the BSE and RPA spectra, besides the redshift, stem from bright and dark exciton solutions of the BSE due to the spin-dependent e-h exchange coupling. The reduction of absorption due to dark excitons is not obtained in a spin-averaged treatment. This is seen in Fig. 2(b), where we compare the BSE spectra of V_C^{2+} as obtained in the two ways.

TABLE II. Ionization (G_0W_0) and excitation (BSE) thresholds as well as experimental data. Also the excitation energy of the transition between the a and e level are given. Values are in eV.

	V_C^{2+}			V_C^+			V_C^0		
	G_0W_0	BSE	E_{eh}	G_0W_0	BSE	E_{eh}	G_0W_0	BSE	E_{eh}
$a \to e$				1.09	0.89	0.20	1.92	1.68	0.24
$V \to a$	1.83	1.65	0.18	2.39	2.16	0.23			
$V \to e$	2.14	1.96	0.18	2.36	2.13	0.23	2.80	2.56	0.21
$a \to C$				1.84	1.61	0.23	2.23	2.02	0.21
Experimental thresholds									
Quenching of V_C^+				1.47 [a]		1.6 [b]			
Restoring of V_C^+				1.81 [a]		1.9 [b]			

[a]Ref. [7].
[b]Ref. [8].

The vertical excitation $a \to e$ between the defect levels occur at 0.89 and 1.68 eV for V_C^+ and V_C^0 well below the onset of transitions involving extended states. An important result is that the transitions to the CB set in at energies (vertical transitions at 1.61 and 2.02 eV for V_C^+ and V_C^0, respectively) below the threshold for excitation from the VB (2.13 eV for V_C^+ and 2.56 eV for V_C^0).

From recent time-resolved photo-EPR experiments [8] cross sections for quenching and restoring of the EPR

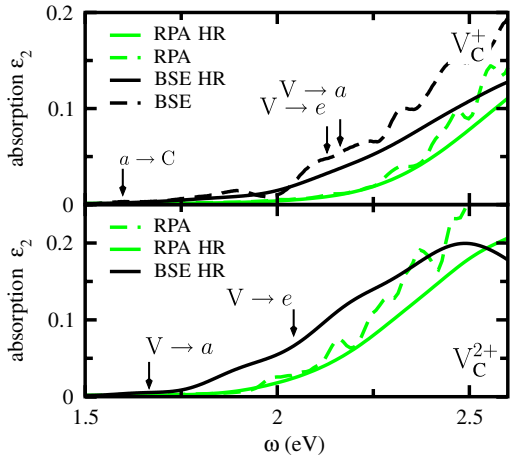

FIG. 3 (color online). Absorption spectra of V_C^+ and V_C^{2+}. G_0W_0-RPA and extrapolated G_0W_0-BSE spectra for high k-point density are shown. Arrows indicate excitation threshold from Table II. The spectra RPA-HR and BSE-HR include Huang-Rhys factors. A broadening of 0.01 eV was used for the raw G_0W_0-RPA spectra.

signal of V_C^+ are available with thresholds at 1.6 and 1.9 eV, respectively. Steady state photo-EPR [7] yields values of 1.47 and 1.81 eV, respectively, (cf. Table II). The calculated onset for excitation $a \rightarrow C$ at 1.61 eV agrees well with the experiments. A rise of the quenching cross section at 2.4 eV [8] should be related to our finding for the onset of the transitions $V \rightarrow a$ at 2.16 eV and direct ionization above 2.4 eV that yields V_C^0. For restoring V_C^+ the excitation of an *e-h* pair with its subsequent thermal dissociation or direct ionization is required with thresholds of 1.65 and 1.83 eV, respectively. The comparison with experiment indicates that direct ionization is the relevant process. Our analysis of competing excitations suggests a reinterpretation of the photo-EPR spectra [6–8] in terms of a photoionization of V_C^+ via V_C^{2+} instead of V_C^0 as considered there. Correspondingly, the ionization levels deduced from the experiments have to be reassigned and corrected for the exciton binding energy.

In summary, we conducted GW + BSE full fledge calculations of the photophysics of the carbon vacancy in 4*H*-SiC. We demonstrate the importance of adding correlation effects at that level, in spite of the fact that the structure is well described at the DFT level. Charge state-dependent corrections include the ionization levels (up to 0.5 eV), the electron-electron repulsion U ($\sim$0.3 eV), and the *e-h* attraction ($\sim$0.23 eV). This has implications for the analysis of defects in materials, such as oxides, where the correct description of the bonding is an issue. We showed that ionization of the defect into V_C^{2+} and V_C^0 compete. However, for the range of photon energies in which photo-EPR experiments identified thresholds only the former ionization channel is active. Excitation spectra are redshifted by strong excitonic effects. This unambiguously rectifies the earlier experimental assignment of transitions and the assessment of ionization levels. These are pivotal for the defect diffusion and for understanding the carrier compensation in semi-insulating SiC.

The authors thank Dr. M. E. Zvanut and Dr. N. T. Son for fruitful discussions. We acknowledge funding by the Deutsche Forschungsgemeinschaft (BO1851/2), Spanish MEC (FIS2007-65702-C02-01), ACI-promciona project (ACI2009-1036), and "Grupos Consolidados UPV/EHU del Gobierno Vasco" (IT-319-07), the European Community through e-I3 ETSF project (Contract No. 211956), and support by the Barcelona Supercomputing Center, "Red Espanola de Supercomputacion."

[1] W. J. Choyke and L. Patrick, Phys. Rev. B **4**, 1843 (1971); L. W. Song, X. D. Zhan, B. W. Benson, and G. D. Watkins, Phys. Rev. B **42**, 5765 (1990).

[2] A. F. Kohan, G. Ceder, D. Morgan, and C. G. Van de Walle, Phys. Rev. B **61**, 15 019 (2000); S. B. Zhang and S. H. Wei, Phys. Rev. Lett. **86**, 1789 (2001); J. Neugebauer and C. G. Van de Walle, Phys. Rev. Lett. **75**, 4452 (1995).

[3] G. Onida, L. Reining, and A. Rubio, Rev. Mod. Phys. **74**, 601 (2002).

[4] M. P. Surh, H. Chacham, and S. G. Louie, Phys. Rev. B **51**, 7464 (1995); Y. Ma and M. Rohlfing, Phys. Rev. B **77**, 115118 (2008); P. Rinke, A. Janotti, M. Scheffler, and C. G. Van de Walle, Phys. Rev. Lett. **102**, 026402 (2009).

[5] M. Rohlfing and S. G. Louie, Phys. Rev. Lett. **80**, 3320 (1998); S. Albrecht, L. Reining, R. Del Sole, and G. Onida, Phys. Rev. Lett. **80**, 4510 (1998); L. Wirtz, A. Marini, and A. Rubio, Phys. Rev. Lett. **96**, 126104 (2006); D. Varsano, A. Marini, and A. Rubio, Phys. Rev. Lett. **101**, 133002 (2008); L. Yang, M. L. Cohen, and S. G. Louie, Phys. Rev. Lett. **101**, 186401 (2008).

[6] M. E. Zvanut and V. V. Konovalov, Appl. Phys. Lett. **80**, 410 (2002).

[7] N. T. Son, B. Magnusson, and E. Janzén, Appl. Phys. Lett. **81**, 3945 (2002).

[8] J. Dashdorj, M. E. Zvanut, and J. G. Harrison, J. Appl. Phys. **104**, 113707 (2008).

[9] M. Bockstedte, M. Heid, and O. Pankratov, Phys. Rev. B **67**, 193102 (2003).

[10] T. Umeda *et al.*, Phys. Rev. B **69**, 121201(R) (2004).

[11] R. Aavikko *et al.*, Phys. Rev. B **75**, 085208 (2007).

[12] Z. Zolnai, N. T. Son, C. Hallin, and E. Janźen, J. Appl. Phys. **96**, 2406 (2004).

[13] A. Marini, C. Hogan, M. Grüning, and D. Varsano, Comput. Phys. Commun. **180**, 1392 (2009).

[14] For the DFT-LSDA ground state, the ABINIT-package [X. Gonze *et al.*, Comput. Mater. Sci. **25**, 478 (2002)] with norm conserving pseudopotentials [N. Troullier and J. L. Martins, Phys. Rev. B **43**, 1993 (1991)], a plane wave basis (energy cutoff of 30 Ry) and, to reduce the defect-defect interaction, the special k point $(0, 0, \frac{1}{4})$ was used. At this k point the highest VB lies 60 meV below the VB edge. Ionization levels and thresholds in Tables I and II were corrected for this and a similar effect in the CB. Tests for cells with 576 lattice sites confirmed DFT results.

[15] G_0W_0 calculations employ the plasmon pole approximation and include local-field effects in the dielectric function ε and self-energy Σ with an energy cutoff of 6 Ry. Convergence was found to be better than 0.1 eV for these parameters and the number of empty bands. QP energies for the paramagnetic V_C^+ and V_C^- and all spectra were evaluated including spin. We employ $\varepsilon(\omega)$ of the defect-free supercell as the transition between the defect levels results in an artificial enhancement of $\varepsilon(\omega = 0)$, which reduces with increasing cell size. Tests show that this leads to an underestimation of QP corrections of about 0.1 eV.

[16] W. G. Aulbur, M. Städele, and A. Görling, Phys. Rev. B **62**, 7121 (2000).

[17] *Semiconductors Physics of Group IV Elements and III-V Compounds*, edited by K. Hellwege and O. Madelung, Landolt-Börnstein, New Series (Springer, Berlin, 1982).

[18] A. Zywietz, J. Furthmüller, and F. Bechstedt, Phys. Rev. B **59**, 15 166 (1999).

[19] The onset of transitions indicated in Fig. 2 reflect the fact that the corresponding spectra are calculated including bands at the special k point only.

[20] To avoid artifacts from the dispersion of defect levels, the values at the special k point were used at all k points.